J Therm Anal Calorim (2012) 107:419–423
DOI 10.1007/s10973-011-1922-x

An indirect thermodynamic model developed for initial stage sintering of an alumina compacts by using porosity measurements

Y. Sarıkaya · M. Önal · K. Ada

Received: 8 October 2010 / Accepted: 16 September 2011 / Published online: 11 October 2011

Abstract The specific micro- and mesopore volumes (V) of alumina compacts fired between 900 and 1250 °C for 2 h were determined from nitrogen adsorption/desorption data. The V value was taken as a sintering equilibrium parameter. An arbitrary sintering equilibrium constant (K_a) was estimated for each firing temperature by assuming $K_a = (V_i - V)/V$, where V_i is the largest value at 900 °C before sintering. Also, an arbitrary Gibbs energy (ΔG_a°) of sintering was calculated for each temperature using the K_a value. The graph of ln K_a versus $1/T$ and ΔG_a° versus T were plotted, and the real enthalpy (ΔH°) and the real entropy (ΔS°) of sintering were calculated from the slopes of the obtained straight lines, respectively. On the contrary, real ΔG° and K values were calculated using the real ΔH° and ΔS° values in the $\Delta G^\circ = -RT \ln K = 165814 - 124.7T$ relation in SI units.

Keywords Adsorption · Alumina · Porosity · Sintering thermodynamics

Introduction

Sintering is densification of a powder compact by firing, which is the last step in ceramic production. Sintering parameters may be divided into two major parts such as material variables and process variables [1]. Main material variables are chemical composition, particle shape, particle size distribution, agglomeration degree, porosity, crystal structure, impurity, and homogeneity of the powder. Process variables include sintering conditions such as compaction type and pressure, atmosphere, temperature, time, firing schedule, etc. Various measurable parameters of a ceramic including porosity, density, crystallinity, hardness, catalytic activity, permeability, adsorptivity, thermal, and electrical conductivity, etc. change depending on both types of variables [2–4]. These variables have been controlled by the ceramics processing. Changes in the measurable parameters with a variable can be only investigated when other variables were kept constant.

Besides different experimental observations, kinetic and thermodynamic studies are the most powerful tools to understand sintering. Kinetic for sintering needs the changes in a measurable parameter only with time, whereas thermodynamics only with temperature at equilibrium conditions. The sintering kinetics has been intensively investigated by many researchers previously [1–8].

Since there are many experimental difficulties in obtaining exact basic thermodynamics data for high-temperature systems, there is lack of intense studies on the sintering thermodynamics. However, various approximate calculations have been made for this phenomenon in the absence of the complete data for exact determinations [9–14]. For this reason, new approaches are required for sintering thermodynamics. Accordingly, the purpose of this study is to develop a thermodynamic model for sintering using porosity measurements.

Y. Sarıkaya · M. Önal (✉)
Department of Chemistry, Faculty of Science, Ankara University, Tandoğan 06100, Ankara, Turkey
e-mail: onal@science.ankara.edu.tr

K. Ada
Department of Chemistry, Faculty of Arts and Sciences, Kırıkkale University, Kırıkkale, Turkey

Experimental

Preparation, compaction, and firing of the alumina powder

An alumina precursor was obtained by homogeneous precipitation from a boiling aqueous solution of 0.20 M Al^{3+} and excess urea. The precursor was calcined at 900 °C for 2 h to yield δ-Al_2O_3 powder. The morphology, particle size distribution, agglomeration degree, crystal structure, adsorptive properties, and initial stage sintering kinetics of the powder used in this study were extensively investigated in our previous studies [15, 16].

Powder compacts with a diameter of 14 mm were prepared using oleic acid (12% by mass) as binder under 32 MPa by a uniaxial press (Graseby/Specac). They were outgassed by heating from room temperature to 900 °C with a heating rate of 10 K min^{-1} and kept at this temperature of 2 h using a furnace (Protherm, Model FFL 120/7, Alser). The outgassed compacts were then fired to different temperatures between 950 and 1250 °C with a heating rate of 5 K min^{-1} and kept at this temperature for 2 h using same furnace. All firings were repeated for 4 h using different compacts. After firing, each compact was cooled spontaneously to room temperature, without any cooling regime.

Nitrogen adsorption on the fired alumina compacts

The adsorption and desorption of nitrogen on all the fired alumina compacts at liquid nitrogen temperature were investigated by a volumetric adsorption instrument [17, 18]. Two repeated measurements were performed for each sample. The instrument was constructed completely of Pyrex glass and connected to high vacuum. Before measurements, each sample was outgassed at 150 °C for 4 h under a vacuum of 10^{-5} mmHg.

The indirect thermodynamic model

Since exact changes in basic thermodynamics quantities such as heat capacity, enthalpy, and entropy are not available during firing, and thermodynamic calculation can not be directly performed by sintering of ceramics and composites. To overcome these obstacles, an indirect thermodynamic model for sintering as well as some other processes was developed in our previous works, on the basis of the following assumption [19–22].

1. The time elapsed during sintering should be sufficient to establish a thermodynamic equilibrium, after which, the values of measurable properties such as porosity, density, and shrinkage of the sintered material do not change.
2. The values of the measurable properties do not change when the sintered material is cooled to room temperature.
3. When the sintering process is at equilibrium, an arbitrary equilibrium constant can be defined using a selected measurable variable.
4. The basic thermodynamic equations should be valid for arbitrary thermodynamic calculations.
5. Temperature dependence of arbitrary and real thermodynamic state functions may be different from each other, but their temperature derivative or slopes of the related straight lines should be the same. An exact match of these lines is not generally expected but if that happens, it may be a sign of the validity of equilibrium constant selected.

Results and discussion

Nitrogen adsorption/desorption isotherms and specific micro- and mesopore volumes

The nitrogen adsorption and desorption isotherms at liquid nitrogen temperature for all fired compacts were examined, and representative ones are shown in Fig. 1. The isotherms show that adsorption capacity decreases with increasing sintering temperature and approaches minimum at 1250 °C. According to Brunauer, the classification of the isotherms is similar to Type II [23, 24]. The shapes of the adsorption and desorption isotherms show that the fired compacts are mainly mesoporous solid but also contain some micropores. The widths of micropores are smaller than 2 nm and mesopores between 2 and 50 nm. The other empty spaces in a solid, the widths of which are larger than 50 nm, are known as macropores. Recently, the pores with the widths between 1 and 100 nm are called nanopores [25]. The radius of a pore, assumed to be cylindrical, can be taken as half of the pore width. The volume of pores in 1 g solid is defined as the specific pore volume.

After respective monomolecular and multimolecular adsorption at the relative equilibrium pressure interval $0 < x < 0.35$ were complete, capillary condensation began, and all micro- and mesopores filled up to $x = 0.96$ [26]. Bulk liquid nitrogen forms at $x = 1$. The liquid nitrogen outside and within the pores evaporates spontaneously as soon as the relative equilibrium pressure by desorption is low enough, at the intervals $1 > x > 0.96$ and $0.96 > x > 0.35$, respectively. The coincidence of the adsorption and desorption isotherms over the interval $0.35 > x > 0$ shows that the multimolecular and monomolecular adsorption are reversible. Capillary condensation begins from the narrowest mesopores and capillary evaporation begins from the largest mesopores. This

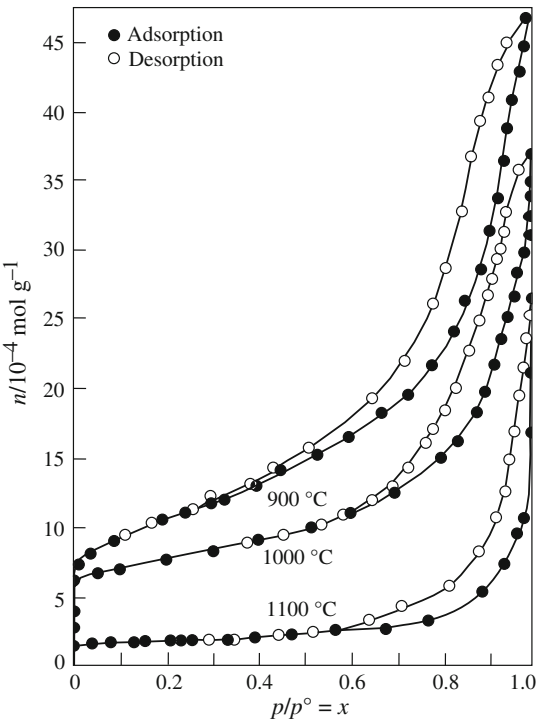

Fig. 1 Adsorption and desorption isotherms of nitrogen at liquid nitrogen temperature for some alumina compacts fired at different temperatures for 2 h (n: adsorption capacity defined as the molar amount of nitrogen adsorbed on 1 g of adsorbent, p: the adsorption and desorption equilibrium pressure, p°: the vapor pressure of bulk nitrogen at experimental temperature, $p/p^\circ \equiv x$: the relative equilibrium pressure)

difference causes the hysteresis between adsorption and desorption isotherms.

The adsorption capacities as liquid nitrogen volume which were estimated from desorption isotherms at $x = 0.96$ are taken as the specific micro- and mesopore volumes of the fired compacts and given in Table 1. It was noticed that the micro- and mesopores are reduced in frequency by increasing the firing temperature but the macropores do not change to a great extent [27]. For this reason, macropore volumes were not determined. Since the specific micro and mesopore volumes of the sintered compacts are not changed by increasing of the firing time from 2 to 4 h, we conclude that the sintering equilibrium is established in the time of 2 h.

Indirect thermodynamic calculations

The specific micro- and mesopore volume (V) is taken as an equilibrium variable for sintering. When the sintering process is at equilibrium, an arbitrary constant (K_a) can be defined using this variable as follows:

$$\text{Residual porosity } (V) \leftrightarrow \text{ Closed porosity } (V_i - V) \quad (1)$$

$$K_a = (V_i - V)/V \quad (2)$$

where V_i is the initial and largest specific micro- and mesopore volumes before sintering of the compacts calcined at 900 °C for 2 h.

The K_a value for each temperature was calculated from Eq. 2. The corresponding arbitrary Gibbs energy ΔG_a° for each temperature was calculated from the relation

$$\Delta G^\circ = \Delta H^\circ - T\Delta S^\circ = -RT\ln K \quad (3)$$

where ΔH° and ΔS° are the enthalpy and entropy changes, respectively, T is the absolute temperature, and R is the universal gas constant. The calculated arbitrary K_a and ΔG_a° values are given in Table 1.

The variation of the K and ΔG with the temperature provides a useful way of determining the enthalpy and entropy changes, respectively. According to Eq. 3, the slopes of the graphs of $\ln K$ versus $1/T$ and ΔG_a° versus T in Figs. 2 and 3 give the real enthalpy (ΔH°) and real entropy (ΔS°) changes for sintering. These quantities were calculated as $\Delta H^\circ = 165814$ J mol^{-1} and $\Delta S^\circ = 124.7$ J K^{-1} mol^{-1}, respectively. Therefore, the initial stage sintering of alumina is of endothermic nature and gives rise to an entropy increase.

The real K and real ΔG° change were calculated for each temperature from Eq. 3 using the calculated ΔH° and ΔS°

Table 1 Temperature dependence of the specific micro- and mesopore volumes (V), arbitrary equilibrium constant (K_a), arbitrary change in Gibbs energy (ΔG_a°), real change in Gibbs energy (ΔG°), and real equilibrium constant (K) for the initial stage sintering of the Al_2O_3 compacts ($\Delta G = -RT\ln K = \Delta H - T\Delta S = 165814 - 124.7T$)

T/°C	T/K	$(1/T)/10^{-4}$ K^{-1}	V/cm^3 g^{-1}	K_a	ΔG°_a/J mol^{-1}	ΔG°/J mol^{-1}	K
900	1173	8.525	$V_i = 0.157$	–	–	–	–
950	1223	8.177	0.120	0.3088	11963	13306	0.2702
1000	1273	7.855	0.102	0.5398	6537	7071	0.5127
1050	1323	7.559	0.071	1.2113	−2108	836	0.9268
1100	1373	7.283	0.052	2.0192	−8021	−5399	1.6048
1150	1423	7.027	0.033	3.7576	−15661	−11634	2.6735
1200	1473	6.789	0.023	5.8261	−21583	−17869	4.3021
1250	1523	6.566	0.022	6.1364	−22972	−24124	6.7100

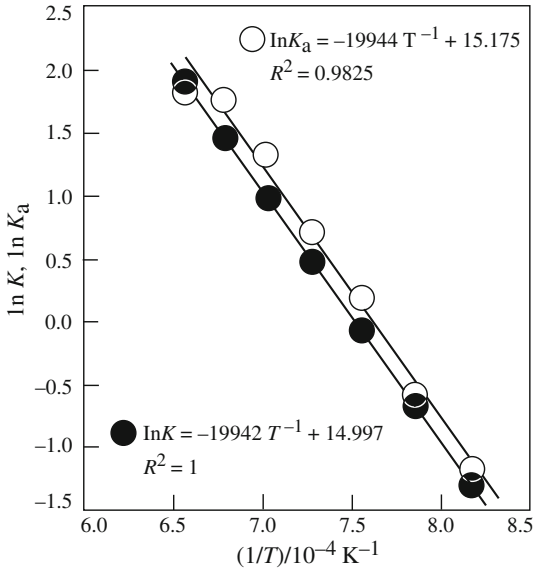

Fig. 2 The van't Hoff plots of the arbitrary and real sintering equilibrium constants (K_a and K)

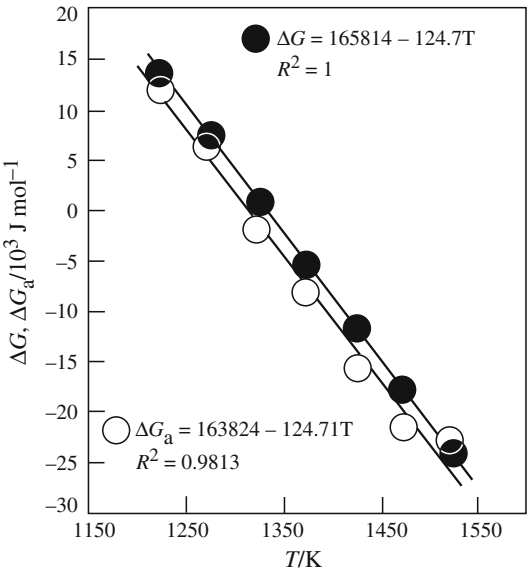

Fig. 3 The variation of the plots of the arbitrary and real Gibbs energy changes (ΔG_a° and ΔG°) as a function of sintering temperature

values, and given in Table 1. The plots of ln$K$ versus $1/T$ and ΔG° versus T are also given in Figs. 2 and 3, respectively. The nearly overlapping of the arbitrary and real straight lines proves the validity of the definition of the arbitrary equilibrium constant. The temperature dependence of the real Gibbs energy and the real equilibrium constant of the initial sintering of the alumina between 950 and 1250 °C given in Fig. 4. The relationship of those may be expressed by the function in SI units:

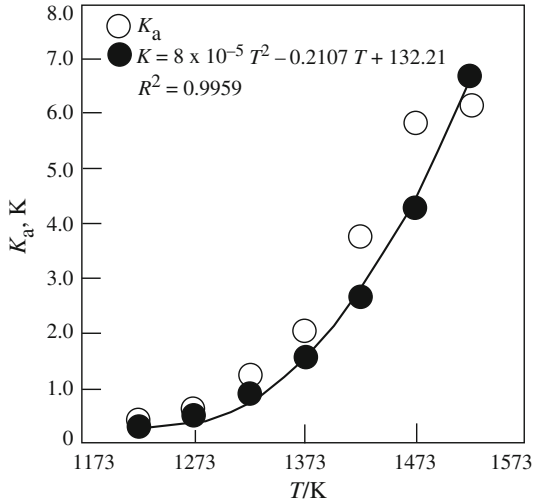

Fig. 4 The variation of the arbitrary and real equilibrium constants (K_a and K) as a function of sintering temperature

$$\Delta G^\circ = -RT\ln K = 165814 - 124.7T. \quad (4)$$

If T is low enough, ΔG° will be positive and the initial sintering will not occur spontaneously. In contrast, when T is high enough, ΔG° will be negative, which means a spontaneous initial sintering process. The similar relationship for same fired compacts was found to be

$$\Delta G^\circ = -RT\ln K = 157301 - 107.6T \quad (5)$$

by taking linear shrinkage instead of specific micro- and mesopore volumes as thermodynamic variable in calculation of the arbitrary equilibrium constant for initial sintering process [19]. The relations are not overlapped but are close to each other. This shows the validity of the developed model for the initial sintering thermodynamics.

Conclusions

Sintering process of compacted ceramic powder could be examined kinetically as well as thermodynamically. Although there are numerous kinetic studies on this process, not enough thermodynamic treatments of such solid phase changes have been reported so far. For this reason, an indirect thermodynamic model has been presented in this study to investigate the sintering process of an alumina powder based upon the specific micro- and mesopore volumes as an equilibrium parameter. It was concluded that by using this parameter and similar ones such as shrinkage and density, the real changes in enthalpy, entropy, and Gibbs energy and also equilibrium constant for sintering can be calculated using well-known basic thermodynamic equations.

Acknowledgements The authors are grateful to the Scientific and Technical Research Council of Turkey for supporting this study under the project TÜBİTAK-106T056.

References

1. Kang SJL. Sintering: densification, grain growth and microstructure. Amsterdam: Elsevier; 2005.
2. Rice RW. Porosity of ceramics. New York: Marcel Dekker; 1998.
3. Rahman MN. Ceramic processing and sintering. 2nd ed. Boco Raton: CRC Taylor and Francis; 2003.
4. Richerson DW. Modern ceramic engineering: properties, processing, and use in design. 3rd ed. Boca Raton: CRC Taylor and Francis; 2006.
5. Perez-Maqueda LA, Criado JM, Real C. Kinetics of the initial stage of sintering from shrinkage data: simultaneous determination of activation energy and kinetic model from a single non-isothermal experiment. J Am Ceram Soc. 2002;85:763–8.
6. Burnham AK. An nth-order Gaussian energy distribution model for sintering. Chem Eng J. 2005;108:47–50.
7. Ada K, Önal M, Sarıkaya Y. Investigation of the intra-particle sintering kinetics of a mainly agglomerated alumina powder by using surface area reduction. Powder Technol. 2006;168:37–41.
8. Kingery WD, Wygant JF. Application of thermodynamics in ceramics: V. Semiempirical calculations. Am Ceram Soc Bull. 1952;31:344–7.
9. Yokokawa H, Kawada T, Dokiya M. Thermodynamic regularities in perovskite and K2NiF4 compounds. J Am Ceram Soc. 1989;72:152–3.
10. Petric N, Martinac V, Tkalčec E, Ivankovič H, Petric B. Thermodynamic analysis of results obtained by examination of the forsterite and spinel formation reactions in the process of magnesium oxide sintering. Ind Eng Chem Res. 1989;28:298–302.
11. Yokokawa H, Sakai N, Kawada T, Dokiya M. Chemical thermodynamic considerations in sintering of LaCrO3-based perovskites. J Electrochem Soc. 1991;138:1018–27.
12. Gross GM, Seifert HJ, Aldinger F. Thermodynamic assessment and experimental check of fluoride sintering aids for AlN. J Eur Ceram Soc. 1998;18:871–7.
13. Subasri R, Mallika C, Mathews T, Sastry VS, Sreedharan OM. Solubility studies, thermodynamics and electrical conductivity in the Th1–*x*Sr–O2 system. J Nucl Mater. 2003;312:249–52.
14. Sarıkaya Y, Ada K, Alemdaroğlu T, Bozdoğan İ. The effect of Al^{3+} concentration on the properties of alumina powders obtained by reaction between aluminium sulphate and urea in boiling aqueous solution. J Eur Ceram Soc. 2002;22:1905–10.
15. Ada K, Sarıkaya Y, Alemdaroğlu T, Önal M. Thermal behavior of alumina precursor obtained by the aluminium sulphate-urea reaction in boiling aqueous solution. Ceram Int. 2003;29:513–8.
16. Sarıkaya Y, Ada K, Önal M. Applications of the zero-order reaction rate model and transition state theory on the intra-particle sintering of an alumina powder by using surface area measurements. J Alloy Compd. 2007;432:194–9.
17. Noyan H, Önal M, Sarıkaya Y. The effect of heating on surface area, porosity and surface acidity of a bentonite. Clays Clay Miner. 2006;54:375–81.
18. Sarıkaya Y, Aybar S. The adsorption of NH3, N2O and CO2 gases on the 5A molecular sieve. Commun Fac Sci Univ Ank. 1978;24B:33–9.
19. Sarıkaya Y, Ada K, Önal M. A model for initial-stage sintering thermodynamics of an alumina powder. Powder Technol. 2008;188:9–12.
20. Noyan H, Önal M, Sarıkaya Y. Thermal deformation thermodynamics of a smectite mineral. J Therm Anal Calorim. 2008;91:299–303.
21. Bayram H, Önal M, Yılmaz H, Sarıkaya Y. Thermal analysis of a white calcium bentonite. J Therm Anal Calorim. 2010;101:873–9.
22. Noyan H, Önal M, Sarıkaya Y. A model developed for acid dissolution thermodynamics of a Turkish bentonite. J Therm Anal Calorim. 2008;94:591–6.
23. Brunauer S, Deming LS, Deming DM, Teller E. On a theory of the van der Waals adsorption of gases. J Am Chem Soc. 1940;62:1723–32.
24. Rouquerol F, Rouquerol J, Sing K. Adsorption by powder and porous solids. London: Academic Press; 1999.
25. Lu GQ, Zhao XS. Nanoporous materials. London: Imperial College Press; 2006.
26. Linsen BG. Physical and chemical aspects of adsorbents and catalysts. London: Academic Press; 1970.
27. Hugo P, Koch H. Production of porous alumina with defined bimodal pore structure. Ger Chem Eng. 1979;2:24–30.